Extended Experimental Procedures

Mice

Rosa-*rtTA:*Tet-O-*Oct4* and ERT-*Cre* transgenic mice were purchased from the Jackson Laboratories. Tet-O-*Myc* transgenic mice were kindly provided by Dr. Yi Li at Baylor College of Medicine. *Ezh2*$^{f/f}$ mice were obtained from the University of North Carolina (UNC)-Mutant Mouse Regional Resource Center (MMRRC) (Su et al., 2003). *PHF20* knockout mice were kindly provided by Dr. Bedford in M.D. Anderson Cancer Center (Badeaux et al., 2012). *Jmjd3* was targeted deletion of exon 15-21 using a Cre-LoxP system. *Jmjd3* globally deleted by crossing *Jmjd3*$^{f/f}$ mice with *Hprt*-Cre mice (Jackson Laboratories, strain 004302). Tet-O-*Sox2*, -*Klf4* and -*PHF20* transgenic mice were generated at Baylor college of Medicine. Two independent transgenic lines for each gene were established and maintained by crossing two founders with C57BL/6 mice. These mice were crossed to rtTA-expressing Tet-O-*Oct4* and Tet-O-*Myc* transgenic mice to generate quintuple-transgenic lines. MEFs expressing *rtTA*, Tet-O-*Oct4*, *Sox2*, *Klf4* and *Myc* were generated by intercrossing transgenic male (expressing Tet-O-*Oct4*, -*Sox2*, -*Klf4* and -*Myc* genes as well as *rtTA-M2*) with transgenic female founders (expressing Tet-O-*Oct4*, -*Sox2*, -*Klf4* and *rtTA*). All the mice were maintained in a pathogen-free animal facility. All animal studies were performed by following the approved protocol of both the Baylor College of Medicine and TMHRI Institutional Animal Care and Use Committee.

Cell Culture

mESCs and miPSCs were cultured in mESC medium (DMEM with 15% FBS, 1 mM L-glutamine (Invitrogen), 1% nonessential amino acids (Invitrogen), 0.1 mM β-mercaptoethanol (Sigma) and 1,000 U ml−1 LIF (Santa cruz)) on irradiated feeder cells.

MEFs were isolated by trypsin digestion of midgestation (E13.5) embryos followed by culture in fibroblast medium (DMEM with 10% FBS, 1 mM L-glutamine, 1% nonessential amino acids and 0.1 mM β-mercaptoethanol). hiPSC culture medium consists of DMEM/F12 with 20% Knockout Serum Replacement (Invitrogen), 1 mM L-glutamine, 0.1 mM mercaptoethanol , 1% non-essential amino acid solution, and 10 ng/mL of FGF2 (Invitrogen).

Lentivirus Transduction

All lentiviral particles were generated as previously described (Peng et al., 2005): 293T cells cultured on T175 flasks were transfected with a lentiviral vector expressing shRNA/cDNA(22.5 μg) together with the packaging plasmids VSV-G (10 μg) and Δ8.9 (15 μg) using lipofectamine 2000 (Invitrogen) transfection reagent. Viral supernatants were collected at 48 h after transfection, yielding a total of ~35 ml of supernatants per virus. Viral supernatants were further concentrated by ~200-fold using ultracentrifugation at 25,000 rpm for 2 h at 4 °C and resuspension in 175 μl of PBS. The MEFs were infected concentrated virus with polybrene (8 μg/ml; Sigma). Typically, more than 90% of cells were successfully transduced using this methodology as judged by a GFP cDNA transduction. The lentiviral shRNAs information can be found in Table S2.

Knockdown of PHF20 During Reprogramming

To determine the function of PHF20 in different reprogramming stages, we knocked down *PHF20* in different time points. We seeded Tet-O-4F M2-11 MEFs on feeder cells on day -1, and then transduced them with *PHF20*-specific lentiviras-based constitutively expressing shRNA on day 0. We changed the culture medium (containing viruses) with fresh ES medium with Dox.

For knockdown at other time points, we infected cells with PHF20-specific or control lentiviral shRNA in ES medium with Dox on day 4, 8 or 12, as indicated. The infected cells were maintained in ES medium with Dox, and AP^+ colonies were counted on day 14.

Cloning of the Full-Length *Jmjd3* and *PHF20* cDNAs and Various Mutants

To clone the full-length *Jmjd3* cDNA, we isolated total RNA and amplified *Jmjd3* cDNA fragments by PCR. The 5 kb PCR product containing the *Jmjd3* was cloned into the HA- or Flag-tagged pcDNA3.1 vector. Truncated deletion mutants were generated by performing PCR with different primers. A similar strategy was used to clone the full-length and truncates of *PHF20*. Sequences of the primers can be found in Table S1. *Jmjd3* H1390A mutation was generated using QuikChange II XL site-directed mutagenesis kit (Agilent technologies). The primers used for cloning are listed in Table S1. All the cDNAs were sequenced to confirm that their sequences are identical to the published ones in the database.

Isolation of ICM and Establishment of ESC Lines

Blastocysts were isolated from $PHF20^{+/-}$ intercrossed pregnant females at E3.5 day and cultured on the gelatin-coated 24-well plates with ESC culture medium. The growth of ICM were monitored and recorded daily. At day 4, ICM were staining with AP-kit. For establishment of the ESC lines, blastocysts at E3.5 day were cultured on 24-well plates with feeder cells in ESC-medium. At day 8, ESCs were isolated from ICM and further grown on feeder cells. These ESCs were continually passaged to P3.

Generation of Chimeric Mice

Fully reprogrammed iPSCs were microinjected into Balb/c blastocysts for chimeric mice performed in Baylor College of Medicine Genetically Engineered Mouse Core. Chimeric mice could be identified by coat color.

Bisulfite Genomic Sequencing Assay

Bisulfite conversion was performed using the Epitect Bisulfite Kit (QIAGEN). Molecules were cloned using the Topo TA Cloning Kit (Invitrogen), according to the manufacturers' instructions.

***Jmjd3* Demethylase Activity Assay**

293T cells were transfected with HA-*Jmjd3* or various HA-*Jmjd3* mutants. Nuclear lysates were collected after 48 h transfection. The *Utx/Jmjd3* H3K27me3 demethylase activity detection Kit (Epigentek) was used to determine *Jmjd3* H3K27me3 demethylase activity.

Immunofluorescence Staining

The cells were cultured on the pretreated cover slips, fixed with 4% PFA and permeabilized with 0.5% Triton X-100. The cells were then stained with primary antibodies to Oct4 (Santa Cruz), SSEA-1 (Abcam) or HA, followed by staining with the respective secondary antibodies conjugated to Texas Red. Nuclei were counterstained with DAPI (Invitrogen). Cells were imaged using a Leica DMI4000B inverted fluorescence microscope equipped with a C350FX camera.

Alkaline Phosphatase Staining

The Alkaline Phosphatase Detection Kit (Vector lab) was used to determine alkaline phosphatase activity according to the manufacturer's instructions.

Immunoprecipitation (IP) and Immunoblot Analysis.

Cells were lysed in low salt lysis buffer or RIPA buffer containing protease inhibitors. Samples were centrifuged at 10,000 g for 10 min and the supernatants were added to a 40 μl anti-HA gel or anti-Flag M2 affinity gel, as previous described (Cui et al., 2010). The samples were IP with specific antibodies over night at 4°C. The beads were then washed five times, eluted with 3×SDS/PAGE loading buffer and boiled for western blot. Endogenous co-IP was performed as described by using antibodies specific for anti-PHF20 (Cell Signaling Technology) followed by incubation with the immobilized protein A/G (Sigma). Chemiluminescent HRP substrate (Millipore) was used for protein detection.

Chromatin Immunoprecipitation (ChIP)-PCR and ChIP-Seq Analyses

ChIP assay was performed according to the Imprint Ultra Chromatin Immunoprecipitation Kit manual (Sigma), Briefly, ESCs and iPSCs were grown to an approximate final count of 1-5×10^7 cells for each reaction. Cells were cross-linked with 1% formaldehyde solution for 10 min at room temperature and quenched with 0.125M glycine. Cells were rinsed twice with 1×PBS. Cells were resuspended, lysed, and sonicated to solubilize and shear crosslinked DNA. The resulting chromatin extract was incubated overnight at 4°C with 10 μg antibody. Next day, each sample was added 15 μl blocked beads and then incubated at 4°C for 1 h. Beads were washed 5 times with RIPA buffer. The complexes were eluted from beads in elution buffer by heating at 65°C. Input DNA (reserved from sonication) was concurrently treated for crosslink reversal. DNA were treated with RNaseA, proteinase K and purified. Primary antibodies used for IP were: PHF20 (Cell Signaling Technology), Wdr5 (Bethyl), mouse/rabbit IgG and RNA Polymerase II

(Sigma). Relative Fold enrichments were calculated by determining the immunoprecipitation efficiency (ratios of the amount of immunoprecipitated DNA to that of the input sample). For ChIP-Seq analysis, a total of 30 ng of immunoprecipitated DNA fragments was used for the ChIP-Seq library construction. Illumina sequencing was performed. Sequencing reads from PHF20, Wdr5 and Polymerase II-pulled down ChIP-Seq libraries were aligned to the mouse mm8 genome using ELAND software. The statistical significance of the fold change was assessed using the MA-plot-based method (Wang et al., 2010).

ChIP-Seq libraries were prepared using standard protocols (available: www.illumina.com). The resulting libaries were sequenced on an Illumina Miseq instrument in two successive runs, and output pooled for each sample for analysis. The resulting sequence output (bases 2-42) were aligned to mouse genome version mm9 using bowtie 0.12.7 (Langmead et al., 2009). Bound peaks were analyzed using QuEST2.4 (Valouev et al., 2008), with standard parameters and specified enrichment of *n-fold*. The resulting genome-wide binding data were analyzed with utilities in the Cistrome portal (Liu et al., 2011). Genome-wide binding patterns were analyzed with CEAS (Shin et al., 2009). Over-represented transcription factor binding motifs were annotated using the seq position to query mouse or human motifs in the TRANSFAC database (Matys et al., 2006). TSS-proximal binding events were analyzed with the Genomatix software suite (http://www.genomatix.com). The bound and unbound genes were based on the significance of enrichment. Gene ontological analysis of proximal binding events was performed using web based bioinformatics database (http://david.abcc.ncifcrf.gov/).

Real-Time Quantitative PCR (real-time PCR)

Complementary DNA was generated from the total RNA of 293T, MEF and iPS cells with

SuperScript II Reverse Transcriptase (Invitrogen), using oligo (dT) as a primer. Gene transcripts were quantified by real-time PCR with SYBR Green real-time PCR SuperMix for the ABI PRISM Instrument (Invitrogen) in an ABI Prism 7000 system (Applied Biosystems). All of the values of the target gene expression level were normalized to *β-actin*. The primers used in real-time PCR can be found in Table S1.

References:

Cui, J., Zhu, L., Xia, X., Wang, H.Y., Legras, X., Hong, J., Ji, J., Shen, P., Zheng, S., Chen, Z.J., *et al.* (2010). NLRC5 negatively regulates the NF-kappaB and type I interferon signaling pathways. Cell *141*, 483-496.

Langmead, B., Trapnell, C., Pop, M., and Salzberg, S.L. (2009). Ultrafast and memory-efficient alignment of short DNA sequences to the human genome. Genome Biol *10*, R25.

Liu, T., Ortiz, J.A., Taing, L., Meyer, C.A., Lee, B., Zhang, Y., Shin, H., Wong, S.S., Ma, J., Lei, Y., *et al.* (2011). Cistrome: an integrative platform for transcriptional regulation studies. Genome Biol *12*, R83.

Matys, V., Kel-Margoulis, O.V., Fricke, E., Liebich, I., Land, S., Barre-Dirrie, A., Reuter, I., Chekmenev, D., Krull, M., Hornischer, K., *et al.* (2006). TRANSFAC and its module TRANSCompel: transcriptional gene regulation in eukaryotes. Nucleic Acids Res *34*, D108-110.

Peng, G., Guo, Z., Kiniwa, Y., Voo, K.S., Peng, W., Fu, T., Wang, D.Y., Li, Y., Wang, H.Y., and Wang, R.-F. (2005). Toll-like receptor 8 mediated-reversal of CD4+ regulatory T cell function. Science *309*, 1380-1384.

Shin, H., Liu, T., Manrai, A.K., and Liu, X.S. (2009). CEAS: cis-regulatory element annotation system. Bioinformatics *25*, 2605-2606.

Valouev, A., Johnson, D.S., Sundquist, A., Medina, C., Anton, E., Batzoglou, S., Myers, R.M., and Sidow, A. (2008). Genome-wide analysis of transcription factor binding sites based on ChIP-Seq data. Nat Methods *5*, 829-834.

Wang, L., Feng, Z., Wang, X., and Zhang, X. (2010). DEGseq: an R package for identifying differentially expressed genes from RNA-seq data. Bioinformatics *26*, 136-138.

Figure Legends

Figure S1. Determination of Effects of Timing of Dox Withdrawal on Tet-O-induced 4F Mediated Reprogramming and Knockdown Efficiency of shRNAs, Related to Figure 1.

(A) Embryos from two mice were harvested at 13.5 d postcoital. Genomic DNA was extracted and subjected to PCR for Tet-O-*Oct4*, Tet-O-*Sox2*, Tet-O-*Klf4*, Tet-O-*Myc* and *rtTA* genotyping with specific primers. Wild-type MEF cells genomic DNA was included as a control. Red rectangles indicated the MEFs used in Figure 1B. M2-11 MEFs were selected for subsequent studies.

(B) MEFs were reprogrammed by lentivirus-based Tet-O-4F (*Oct4*, *Sox2*, *Klf4* and *Myc*, OSKM) in the presence of Dox, followed by Dox withdrawal at different time points (i.e. day 4, 6, 8, 12 or 14), as indicated. Cells were stained for AP on day 16 to determine the number of AP^+ positive colony.

(C) Tet-O-4F transgenic MEFs were cultured in the presence of Dox, followed by Dox withdrawal at indicated time points. AP positive colonies were counted on day 16.

(D) *Oct4-GFP* reporter MEFs were reprogrammed by lentivirus-based 4F in the presence of Dox, followed by Dox withdrawal at indicated time points. AP^+/GFP^+ colonies were analyzed at day 14 by FACS.

(E) 293T cells were transfected with the shRNA for 12 h, and then were transfected with indicated Flag- or HA-tagged genes for 48 h. Knockdown efficiency was analyzed by western blot.

(F) MEFs were transduced with the lentivirus-mediated shRNA for 48 h, and total RNAs were extracted for real-time PCR analysis.

The data in panels in **B**, **C** and **F** are presented as means ± SD of three independent experiments. N.S. stands for no significant difference between groups by Student's t test. Red rectangles indicated the shRNAs used in Figure 1H.

Figure S2. Analysis Expression of Specific Epigenetic Genes in Mouse and Human Fibroblast Cells, iPSCs and ESCs, Related to Figure 3.

(A) Real-time PCR analysis of *Ink4a*, *Arf* and *p21* expression in WT and *Jmjd3*-deficient MEFs (at passages 1, 3 or 5).

(B) Determination of *Ink4a/Arf* and *p21* shRNA knockdown efficiency by real-time PCR. Red rectangles indicated the shRNAs used in Figure 3D.

(C) H3K27me3 demethylase activity of *Jmjd3* WT and mutants. 293T cells were transfected with HA-*Jmjd3* or various HA-*Jmjd3* mutants. Nuclear lysates were used for H3K27me3 demethylase activity assay.

(D and E) Expression of 59 epigenetic genes in mouse (D) or human (E) fibroblast cells, iPSCs and ESCs was determined by real-time PCR analysis.

(F) Venn diagram shows that 7 genes are commonly and highly expressed in mouse and human iPSCs/ESCs.

The data in (**A**-**C**) are reported as means ± SD of three independent experiments. Asterisks indicate significant differences between groups (*$p < 0.05$, **$p < 0.01$, by Student's t test).

Figure S3. *PHF20* Expression in WT and *Jmjd3*-deficient MEFs and Mouse Tissues, Related to Figure 3.

(A) Real-time PCR analysis of *PHF20* mRNA expression in WT and *Jmjd3*-deficient MEFs (at passage 2). *P* value > 0.05 indicates no significant difference between groups determined by Student's t test.

(B) ChIP-qPCR analysis of H3K27me3 mark of the *PHF20* promoter in WT and *Jmjd3*-deficient MEFs and derived iPSCs. Numbered black bars indicate primer locations (top panel). Data are reported as fold enrichment relative to input DNA.

(C) Real-time PCR analysis of *PHF20* mRNA expression in different mouse tissues.

(D) Western blot analysis of PHF20 protein in different mouse tissues.

The data in (**A**-**C**) are presented as means ± SD from three independent experiments.

Figure S4. PHF20 Plays Important Role in Generation and Maintenance of ESCs and in Cellular Reprogramming, Related to Figure 4.

(A) Determination of *PHF20* shRNA knockdown efficiency by western blot analysis.

(B) Real-time PCR analysis of *PHF20*, *Oct4* and *Nanog* expression in iPSCs treated with 1 μM RA and LIF withdrawal at different time points. All data are normalized to *β-actin* and shown relative to day 0.

(C) Western blot analysis of PHF20 expression in iPSCs treated with 1 μM RA and LIF withdrawal at different time points.

(D) Blastocysts obtained from the heterozygous ($PHF20^{+/-}$) intercrossing were grown in ES cell medium. 5 $PHF20^{+/+}$ and 3 $PHF20^{-/-}$ blastocysts were identified by PCR genotyping. All 5 $PHF20^{+/+}$ blastocysts showed the growth of inner cell mass, while all 3 $PHF20^{-/-}$ blastocysts

were differentiated. Similar results were obtained in two independent experiments. AP staining was performed at day 4. Scale bars, 50 μm.

(E) Bright-field images, AP Staining and immunostaining with antibodies against Nanog and Oct4 in ESCs from *PHF20*$^{+/+}$ blastocytes and cells from *PHF20*$^{-/-}$ blastocysts. DAPI staining for nuclei DNA served as a control. Scale bars, 50 μm. ESC lines were established from *PHF20*$^{+/+}$ blastocytes, but no ESC lines could be established from *PHF20*$^{-/-}$ blastocysts. Similar results were obtained in two independent experiments.

(F) Real-time PCR analysis of *Oct4* and *Cdx2* expression in *PHF20*$^{+/+}$ ESCs and *PHF20*$^{-/-}$ blastocyst-derived cells.

(G) Determination of human *Jmjd3* and *PHF20* shRNA knockdown efficiency by real-time PCR analysis. Red rectangles indicated the shRNAs used in Figure S4I.

(H) AP^{+} colonies were counted on day 30 in 4F-mediated reprogramming of human foreskin fibroblast cells transduced with *Jmjd3*-specific, *PHF20*-specific or control shRNA.

(I) Growth property of WT, *Jmjd3*-deficient, *PHF20*-deficient and double deficient MEFs.

(J) Growth property of *rtTA*-expressing WT and Tet-O-*PHF20* transgenic MEFs with or without Dox treatment.

(K) Bright field images of ESCs. ESCs were infected with *rtTA*/mock or *rtTA*/Tet-O-*PHF20* lentiviruses, and then were subjected to Dox treatment and LIF withdrawal from ES medium for 3 days.

(L) Western blot analysis of PHF20, Oct4, Sox2 and Nanog expression between WT and Tet-O-*PHF20* expressing ESCs after LIF withdrawal up to 3 days.

(M) AP^{+} colonies were counted at day 14 in Tet-O-*PHF20* transgenic MEFs reprogrammed by different combination of 4F.

The data in panels **B**, **F-J**, and **M** are plotted as means ± SD of three independent experiments. Asterisks indicate significant differences between groups (*p < 0.05, **p < 0.01, by Student's t test).

Figure S5. Jmjd3 Interacts with PHF20 and Mediates its Degradation, Related to Figure 5.

(A) Subcellular localization of PHF20 and Jmjd3. 293T cells were transiently transfected with HA-*Jmjd3* and *GFP-PHF20*. The cells were fixed and immunostained with anti-HA and Texas Red-labeled anti-mouse antibodies for HA-*Jmjd3* detection. Scale bars, 10 μm.

(B) ESCs and iPSCs cell fraction extracts were collected and immunoblotted with indicated antibodies.

(C) 293T cells were transfected with Flag tagged *PHF20* truncates and HA tagged *Jmjd3* truncates as indicated. Cell extracts were immunoprecipitated with anti-Flag beads, followed by immunoblot (IB) with a HA antibody.

(D) 293T cells were transfected with Flag-*PHF20* and HA-tagged *Jmjd3*, *Utx* and *Uty*. Cell extracts were immunoprecipitated with anti-Flag beads, followed by IB with a HA antibody.

(E) Jmjd3 induces PHF20 degradation. 293T cells were transfected with Flag-*PHF20* and increasing doses of HA-*Jmjd3*. PHF20 expression was determined by western blot analysis.

Figure S6. Identification of Trim26 as a PHF20 E3 Ubiquitin Ligase by shRNA library Screening and its Role in Cellular Reprogramming, Related to Figure 6.

(A) 293T cells were transfected with HA-*Jmjd3* and a human E3 ubiquitin ligase shRNAs sublibrary, which targets the Trim family for knockdown. Cell extracts were immunoblotted with anti-*PHF20* and anti-*β-actin*. Quantitative analysis of band density was done. All data are normalized to β-actin and shown relative to the control shRNA transfected samples.

(B) Representative data of western blot analysis of the E3 ligase shRNA screening.

(C) Efficiency of 2 human *Trim26* shRNA knockdown was determined by western blot analysis.

(D) Efficiency of 3 murine *Trim26* shRNA knockdown was determined by western blot analysis.

(E) WT and *PHF20*-deficient MEFs transduced with *Trim26* shRNA along with *Jmjd3* overexpression. Whole-cell extracts were immunoprecipitated with a PHF20 antibody, followed by IB with indicated antibodies.

(F and G) Tet-O-4F transgenic MEFs were transduced with *Trim26, Jmjd3* or specific shRNAs as indicated. Cells were reprogrammed in the presence of Dox for 12 days. AP-positive colonies were counted on day 14.

(H) Quantification of PHF20 protein in WT and *Jmjd3*-deficient MEFs during cellular reprogramming.

(I and J) WT MEF cells were transduced with Tet-O-*Jmjd3* or Tet-O-*Trim26* as indicated. Cells were reprogrammed by lentivirus-based Tet-O-4F in the presence or absence of MG132. On day 6 the cell extracts were collected and immunoblotted with indicated antibodies (I). AP-positive colonies were counted on day 14 (J).

The data in panels **F**, **G**, **H** and **J** are reported as means ± SD of three independent experiments. Asterisks indicate significant differences between groups (*$p < 0.05$, **$p < 0.01$, by Student's t test).

Figure S7. PHF20 is Required for Reactivation of Endogenous *Oct4* Expression in Reprogramming, and Binds to the *Oct4* Promoter, Related to Figure 7.

(A) WT and *PHF20* KO MEFs were reprogrammed by lentivirus-based Tet-O-4F in the presence of Dox for 14 days. Real-time PCR analysis of endogenous *Oct4*, *Sox2*, *Nanog* and other ES genes was performed on day 14.

(B) WT and *PHF20*-deficient MEFs were reprogrammed by lentivirus-based Tet-O-4F in the presence of Dox for all the time, or followed by Dox withdrawn on day 10 and/or transduced with retroviral based *Oct4* overexpression. Cells were stained for AP on day 14 to determine the number of AP positive colony.

(C) ChIP-PCR analysis of PHF20 occupancy at *Oct4, Sox2, Nanog, Esg1, Eras, Rex1, Cripto* and *Dnmt3l* locus. Rabbit IgG ChIP as a negative control.

(D) Interaction of PHF20 with Oct4, Sox2 or with Nanog. 293T cells were transfected with Flag-*PHF20* and *Oct4* (left), *Sox2* (middle) or *Nanog* (right). Cell extracts were immunoprecipiated with anti-Flag beads, followed by IB with indicated antibodies.

(E). ChIP-seq analysis revealed that both PHF20 and Wdr5 bound to the *Oct4* gene, but not to *Sox2* or *Nanog* gene in ESCs and iPSCs.

(F) Venn diagram showing overlap of PHF20- (red) and Wdr5-bound (blue) genes.

(G) Percentage distribution of ChIP-seq binding regions relative to nearest Refseq genes for PHF20 and Wdr5.

(H) Distribution of PHF20 and Wdr5 peaks in a 7 kb region from -2 kb to +5 kb around TSS (indicated by arrow) of genes co-bound by PHF20 and Wdr5. Y-axis, percentage of peaks relative to total peaks within the defined region. X-axis, bin numbers, with each representing a 500 bp region.

(I) GO term analysis for genes bound by PHF20 (left panel) and genes co-bound by PHF20 and Wdr5 (right panel). Selected developmental pathways related GO terms are presented.

The data in panels **A** and **B** are reported as means ± SD of three independent experiments. Asterisks indicate significant differences between groups (*$p < 0.05$, **$p < 0.01$, N.S., not significant, by Student's t test).

Supplemental Figure

Figure S1 (Related to Figure 1)

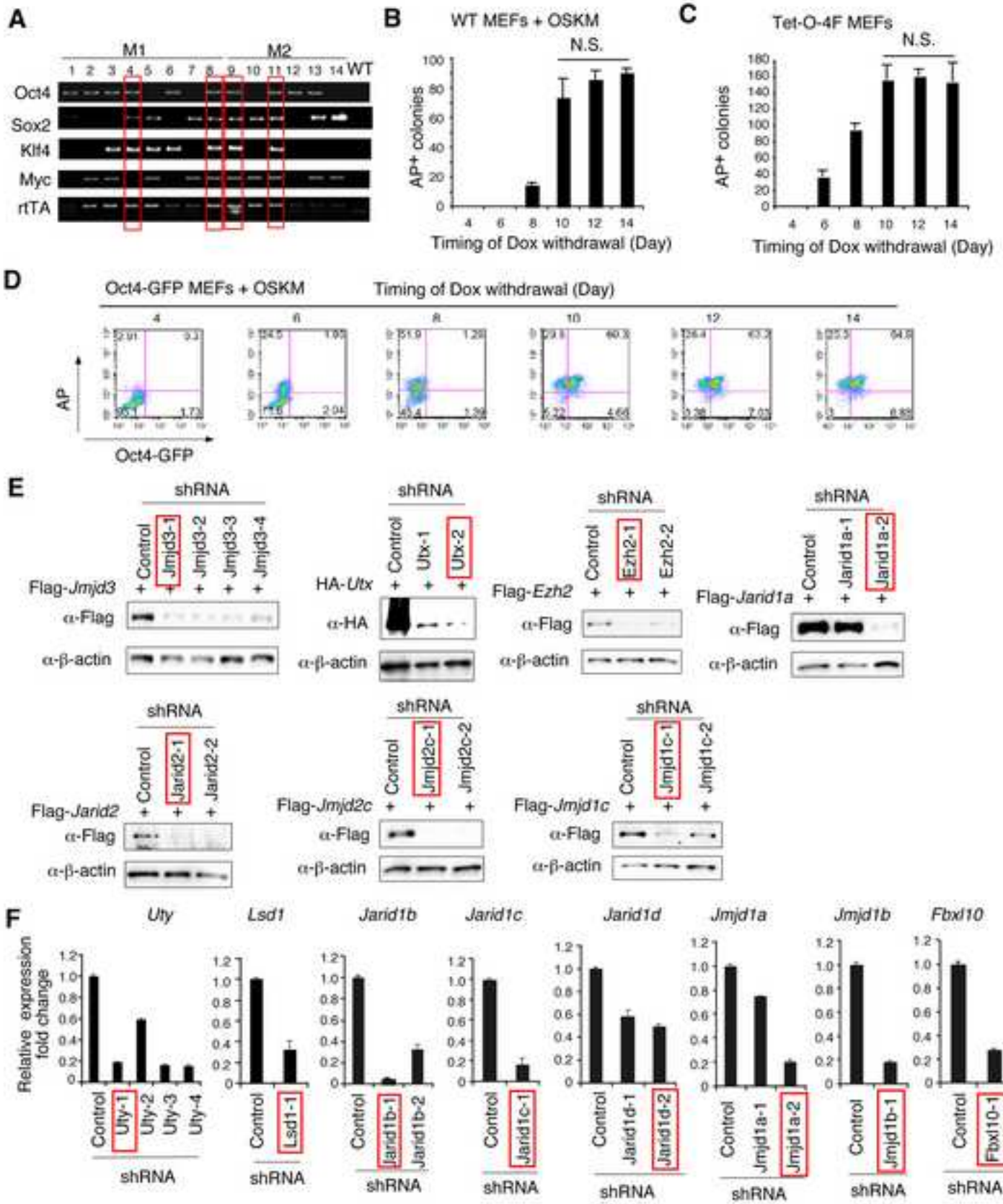

Supplemental Figure 2

Figure S2 (Related to Figure 3)

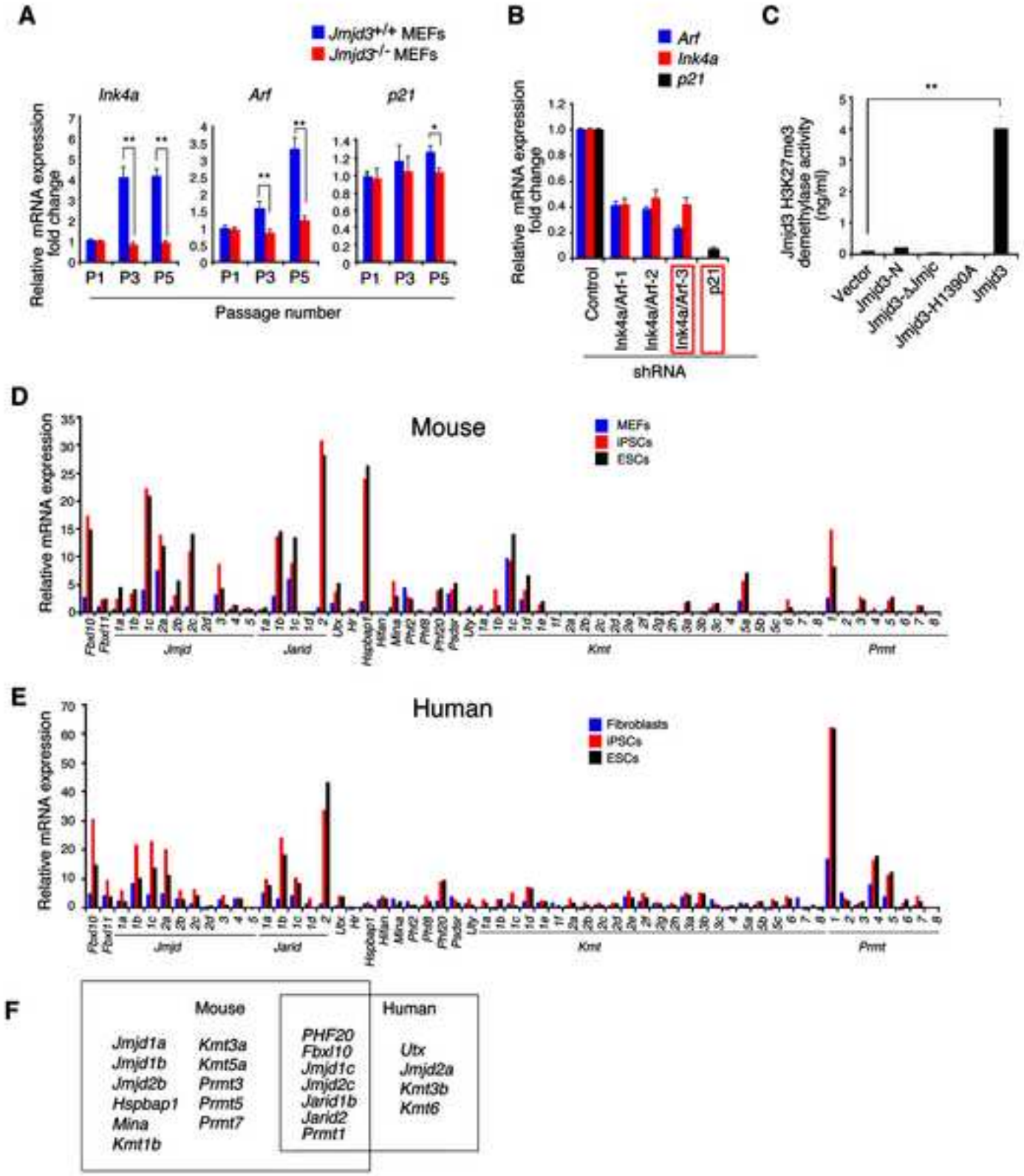

Supplemental Figure 3

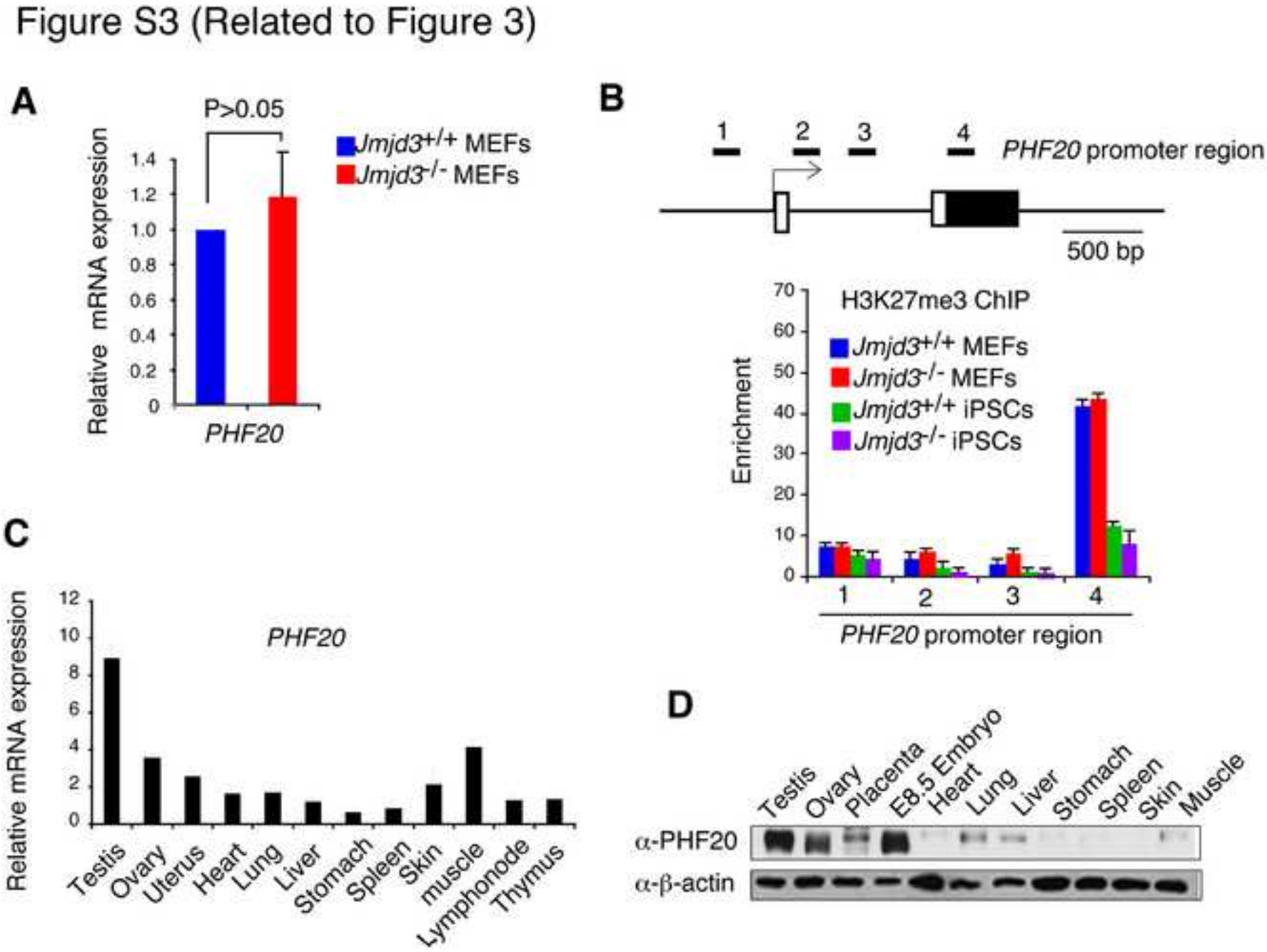

Supplemental Figure 4

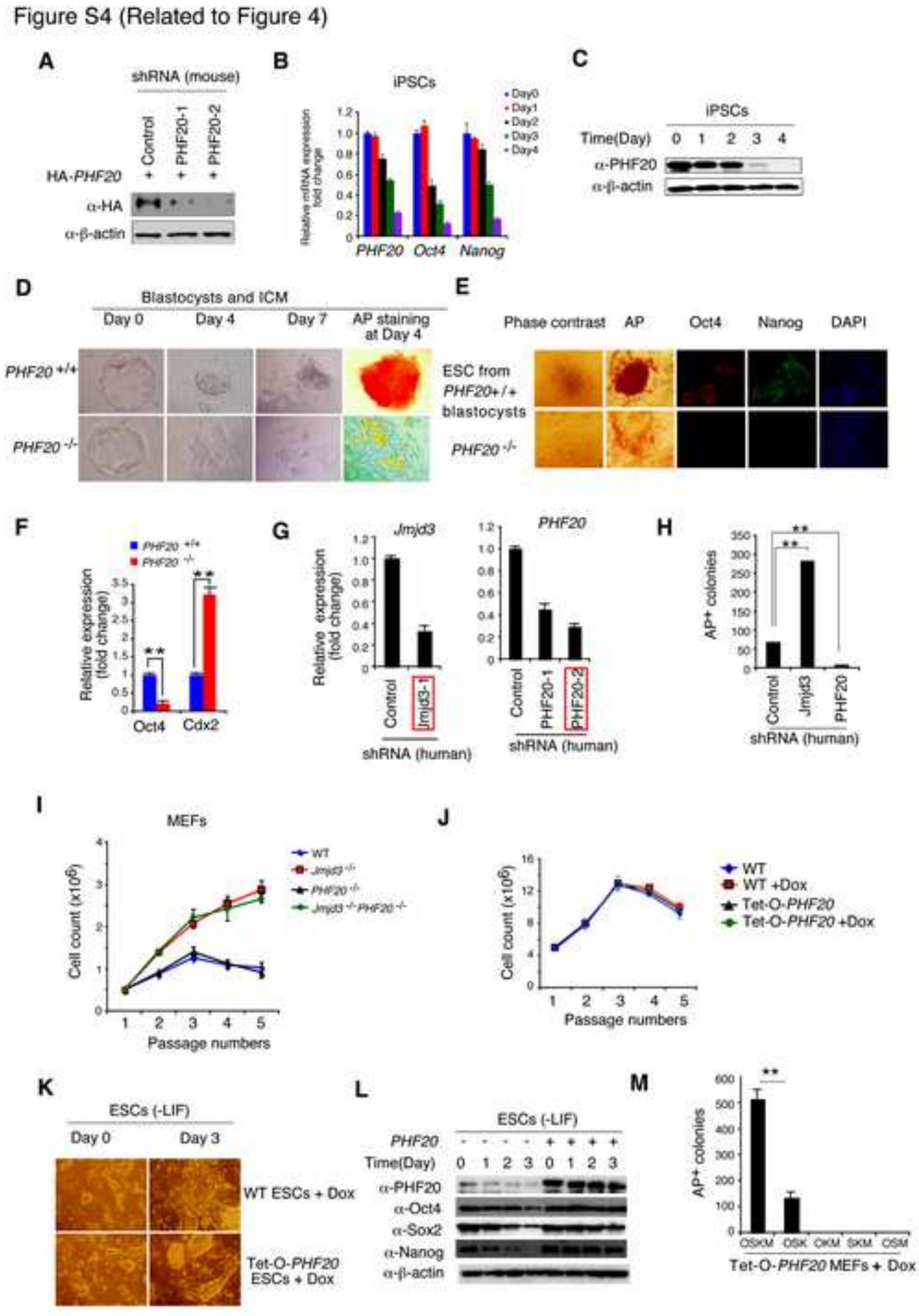

Supplemental Figure 5

Figure S5 (Related to Figure 5)

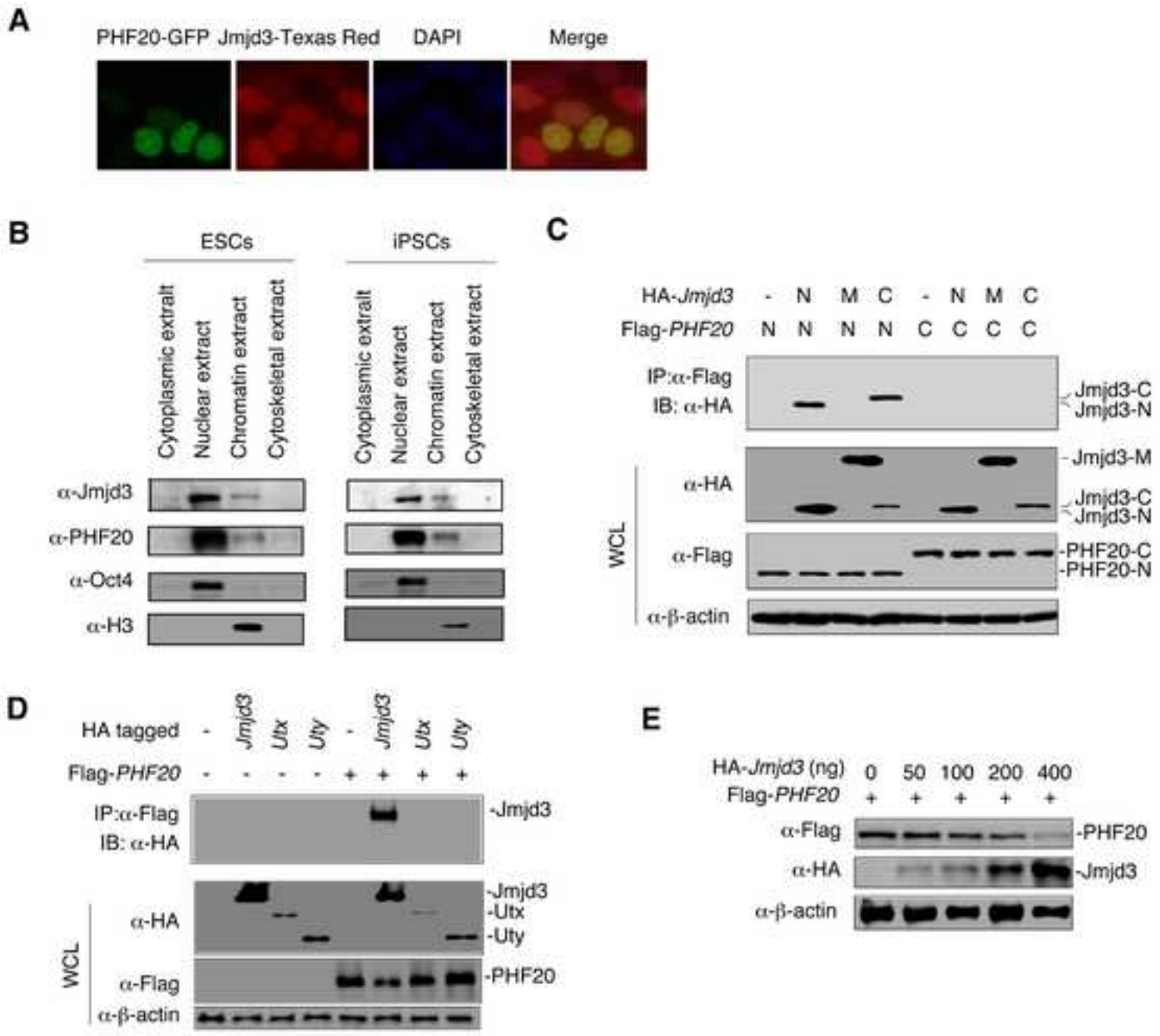

Supplemental Figure 6

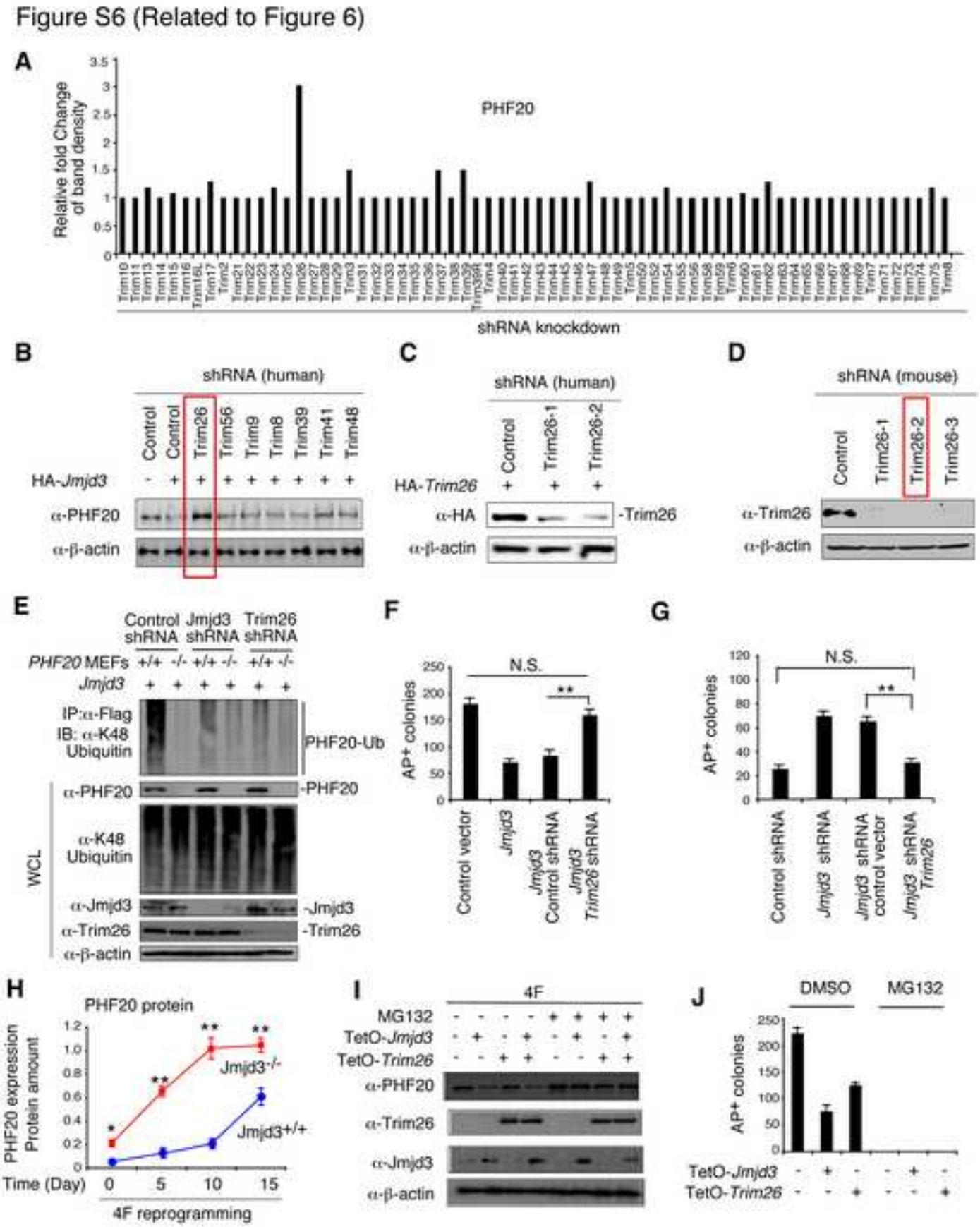

Supplemental Figure 7

Figure S7 (Related to Figure 7)